A Scanning Tunneling Microscopy Study of Ultrathin Film Rutile TiO2(110) Supported on W(100)−O(2 x 1)

ARTICLE *in* THE JOURNAL OF PHYSICAL CHEMISTRY C · DECEMBER 2013

Impact Factor: 4.77 · DOI: 10.1021/jp409948u

4 AUTHORS, INCLUDING:

David Grinter
Brookhaven National Laboratory
15 PUBLICATIONS **101** CITATIONS
SEE PROFILE

Jai Matharu
University College London
3 PUBLICATIONS **14** CITATIONS
SEE PROFILE

THE JOURNAL OF PHYSICAL CHEMISTRY C

Article

pubs.acs.org/JPCC

A Scanning Tunneling Microscopy Study of Ultrathin Film Rutile TiO_2(110) Supported on W(100)-O(2 × 1)

Chi L. Pang, David C. Grinter, Jai Matharu, and Geoff Thornton*

Department of Chemistry and London Centre for Nanotechnology, University College London, 20 Gordon Street, London WC1H 0AJ, United Kingdom

ABSTRACT: Ultrathin films of rutile TiO_2(110) have been grown on a W(100)-O(2 × 1) surface and characterized with a combination of scanning tunneling microscopy (STM) and low-energy electron diffraction (LEED). LEED shows the presence of two orthogonal rotational domains of rutile TiO_2(110). In line with this, STM images reveal that the rutile TiO_2 grows as discrete islands and can be aligned in either of the principal directions of the underlying substrate W(100)-O(2 × 1). High-resolution STM images reveal atomic-scale rows and the presence of point defects on the rutile islands that are characteristic of the native rutile TiO_2(110)-(1 × 1).

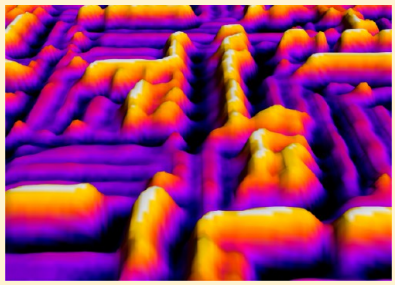

1. INTRODUCTION

Ultrathin metal oxide films supported on conducting substrates are an important class of materials that have received a great deal of attention for a number of reasons. By using such films as mimics of their insulating counterparts, some of the experimental difficulties that arise from studying insulators can be circumvented.[1−5] At the other end of the scale, interaction of the oxide film with the substrate may lead to novel nanostructures with different properties.[6]

TiO_2 is extensively studied on account of its technological importance in applications such as solar cells and self-cleaning surfaces.[7] As the most stable rutile termination, most attention has been focused on the (110) surface.[8−10] Despite this, there are only a few studies of ultrathin rutile TiO_2(110) films.[11−22] This is in part because the native rutile crystal can be made semiconducting by reduction so that charged-particle techniques including scanning tuneling microscopy (STM) already can be used. Nevertheless, there are some cases where an ultrathin film of rutile TiO_2(110) is highly desirable. For instance, limiting the thickness of the rutile film to a few layers allows bulk techniques such as electron paramagnetic resonance (EPR)[5] and resonant inelastic X-ray scattering to be applied in a surface-sensitive manner.[23]

Previously, ultrathin films of rutile TiO_2(110) have been grown on $Ni_{94}Ti_6$(110),[11] Ni(110),[12−15] Mo(110),[16,17] Ag(100),[18] and W(100).[19−22] Although point defects have been imaged only with Ni(110) as the substrate,[12,14] in nearly all the other STM studies the (1 × 1) rows of TiO_2(110) have been observed.[17,18] The exception to this is the case of the film grown on W(100), where STM data were recorded from samples that had been exposed to the atmosphere.[20] As such, while the STM data reveal that the TiO_2(110) grows as islands, no details of the atomic-scale structure were revealed.[20]

Here, we report the characterization of rutile TiO_2(110) ultrathin films supported on W(100)-O(2 × 1) using STM and low-energy electron diffraction (LEED), both within the same vacuum chamber. Results from both techniques indicate that rutile grows in two orthogonal rotational domains. The STM images also show that rutile grows as discrete islands rather than forming a continuous film. In high-resolution images, the TiO_2(110) (1 × 1) rows are imaged together with the characteristic point defects. These high-resolution images show that the atomic-scale structure is indistinguishable from the native TiO_2(110) surface.

We employ W(100)-O(2 × 1) as our substrate as its preparation requires much lower temperatures; previous work indicates that identical TiO_2(110) films are formed whether clean W(100) or W(100)-O(2 × 1) is used.[19,21] Figure 1 shows a ball model of W(100) drawn to scale alongside the W(100)-O(2 × 1) and TiO_2(110) surfaces. W(100) is well-suited to act as a substrate on which to grow TiO_2(110) because it is almost lattice-matched. It is also nonmagnetic, which is crucial for spin-sensitive applications and techniques such as EPR. The W(100)-O(2 × 1) surface is formed by removing (or adding) alternate rows of W along [001], creating {110} microfacets as shown in the model in Figure 1b. O is then adsorbed into the 3-fold hollow sites of the newly created {110} microfacets.[24−26] As the same surface can be formed by removing a row of W along [010], the O(2 × 1) surface forms orthogonal rotational domains. The perfect TiO_2(110) surface is characterized by 5-fold coordinated Ti (Ti_{5c}) rows that alternate with bridging oxygen (O_b) rows. After sample preparation, this surface is decorated with bridging oxygen vacancies (O_b-vac) and bridging hydroxyls (OH_b), the latter resulting from reaction of the O_b-vacs with water residual in the vacuum.[8−10]

Received: October 7, 2013
Revised: November 1, 2013

   dx.doi.org/10.1021/jp409948u | J. Phys. Chem. C XXXX, XXX, XXX−XXX

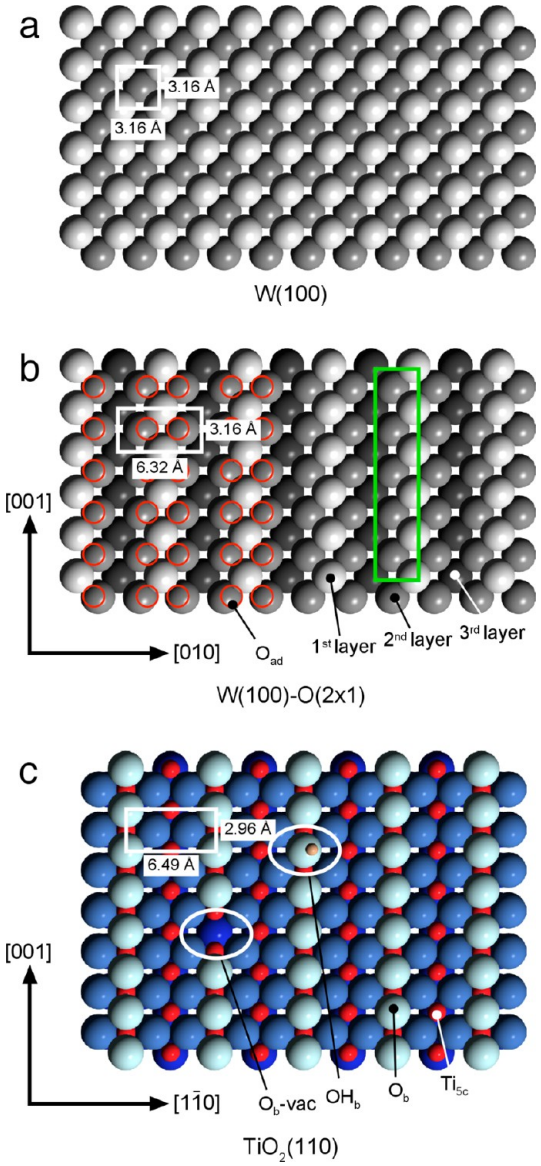

Figure 1. Top view of ball models for (a) W(100), (b) W(100)-O(2 × 1), and (c) TiO_2(110)-(1 × 1) to scale. In (a), two layers of W are visible with the top layer shaded lighter. The W(100)-O(2 × 1) structure in (b) is constructed by removing every other row of W from the top layer in the [001] direction. This exposes a third layer of W, colored black in the model, and creates {110} microfacets, one of which is highlighted with a green rectangle. On the left-hand side, oxygen (O_{ad}) is adsorbed into the 3-fold hollow sites of the {110} microfacets and highlighted as open red circles. In (c), oxygen is shaded blue with the bridging oxygen atoms (O_b) shown lighter. Ti is shown in red, and one of the 5-fold coordinated Ti species (Ti_{5c}) is indicated, as are a bridging oxygen vacancy (O_b-vac) and a bridging hydroxyl (OH_b).

2. EXPERIMENTAL PROCEDURE

The STM data were recorded using two Omicron UHV systems: an AFM/STM and a variable temperature STM. Both consist of an analysis chamber that contains the microscope and a preparation chamber where the films were grown. Both instruments also contain ancilliary devices that allow LEED and Auger electron spectroscopy (AES) measurements. The W(100) substrate (Surface Preparation Laboratory) was prepared by repeated cycles of argon sputtering and annealing to 1050−1150 K in 5×10^{-9} to 5×10^{-8} mbar O_2 and 1400 K in UHV followed by flashing to ∼1500−1600 K in UHV until a well-ordered W(100)-O(2 × 1) pattern was observed in LEED and any contamination was below the detection limit of AES. Ti was deposited on the surface at room temperature from the vapor of a metal wire (Goodfellow) heated by electron bombardment using both home-built and commercial evaporators (Omicron EFM). The sample was then annealed in 1−5 × 10^{-7} mbar O_2 for 1−2 h at 800−850 K and for 0−10 min at 900−1000 K in UHV until a rutile TiO_2(110) pattern was observed in LEED. Temperatures were measured with an optical pyrometer, and sample heating was accomplished via electron bombardment.

STM images were collected in the empty-states regime at room temperature using etched tungsten or mechanically formed PtIr tips. Film coverages are given in monolayer equivalents (MLE), where a monolayer corresponds to the complete coverage of the W(100) substrate by a single continuous rutile TiO_2(110) layer, calculated from the thickness and surface area fraction measured in STM. The z-piezo was calibrated by setting the height of a native TiO_2(110) step at 3.25 Å, the ideal bulk-truncated height.

3. RESULTS AND DISCUSSION

Figure 2 shows a photograph of a LEED pattern recorded from a ∼2.3 MLE film on W(100)-O(2 × 1). A series of schematic, simulated LEED patterns are drawn to scale alongside the photograph. Figure 2a shows the simulated W(100)-(1 × 1) LEED pattern which consists of an array of spots arranged in squares. In Figure 2b, two orthogonal rectangular domains are shown which correspond to the two rotational domains of the W(100)-O(2 × 1) structure. In Figure 2c,d two rotational domains of the simulated TiO_2(110) LEED pattern are shown, and in Figure 2e all the simulated LEED patterns are superimposed. As can be seen, the combined simulated LEED pattern matches almost exactly with the LEED photograph in Figure 2f. This shows that the rutile TiO_2(110) forms in two orthogonal domains as reported previously.[19−22] Also, because the simulations were performed using lattice parameters from the perfect crystal structures of tungsten and rutile TiO_2, the LEED shows that there is either very little or no compression or expansion of the TiO_2(110) lattice in the ultrathin film. Previously published LEED patterns were taken from thicker films so that the substrate spots could not be clearly distinguished.[19,22]

STM images of a W(100)-O(2 × 1) surface are shown in Figure 3 after a small quantity of the oxide film has been grown on it. Apart from the oxide islands, the image is similar to those published for the clean W(100)-O(2 × 1) surface,[25] being characterized by rows aligned either in the W[001] or W[010] directions. Rows in each direction comprise the different rotational domains which are up to ∼150 Å in length. As for the oxide islands, it can be seen that these also grow in orthogonal rotational domains. X-ray photoelectron spectroscopy (XPS) measurements indicate that at low oxide coverages these islands contain about 5−8% reduced Ti^{3+} states, which would correspond to TiO_x ($x \approx 1.960$−1.975).[19,22] However, the presence of reduced Ti species may also be due to electron charge transfer from the substrate W(100)-O(2 × 1) to the film.[21] Close inspection of the islands reveals that they are composed of atomic-scale rows that extend in the same direction as the underlying W(100)-O(2 × 1) rows. These rows have a similar periodicity to the W(100)-O(2 × 1) (6.3 Å), and

dx.doi.org/10.1021/jp409948u | J. Phys. Chem. C XXXX, XXX, XXX−XXX

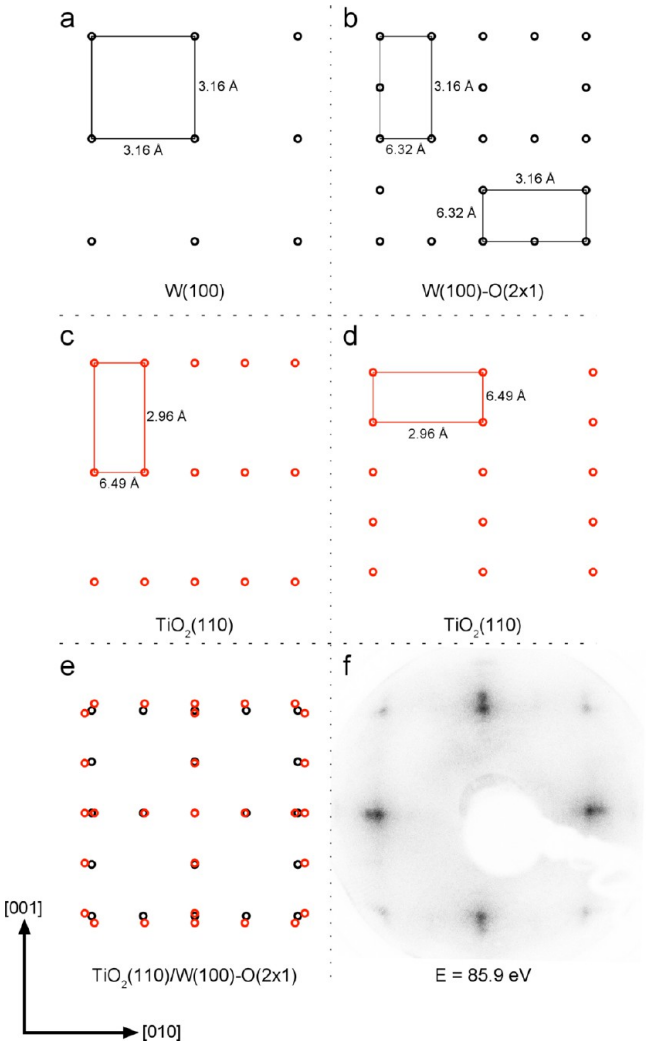

Figure 2. Simulated LEED patterns for (a) W(100), (b) two rotational domains of W(100)-O(2 × 1), (c,d) two rotational domains of TiO_2(110)-(1 × 1), and (e) a composite of the patterns in (a–d). (f) A LEED (energy = 85.9 eV) photograph of a ~2.3 MLE TiO_2(110)-(1 × 1) film grown on W(100)-O(2 × 1). All patterns are to scale, including the photograph, and unit cell sizes refer to real space distances. The crystal directions of W(100) are indicated.

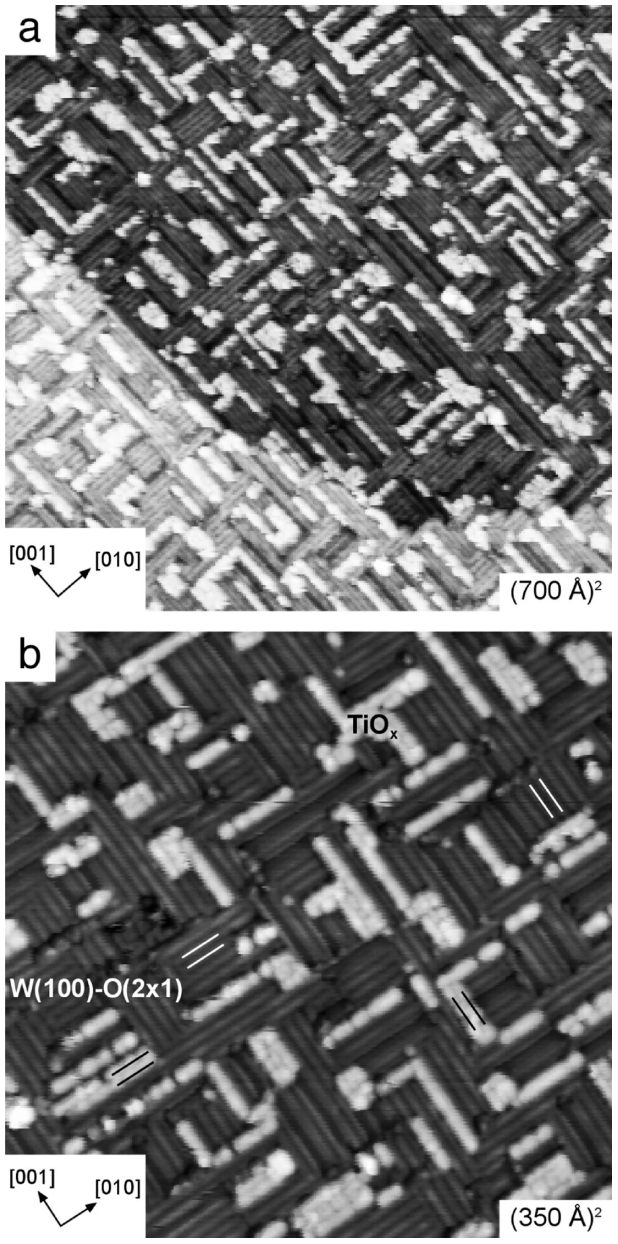

Figure 3. STM images of a ~0.2 MLE film of TiO_x(110) on W(100)-O(2 × 1). (a) (700 Å)^2 image taken at 2.0 V and 0.2 nA. (b) (350 Å)^2 image taken at 1.5 V and 0.5 nA. In (b), an area of TiO_x(110) and an area of the W(100)-O(2 × 1) substrate are indicated. White lines are drawn over some of the W(100)-O(2 × 1) rows then duplicated, in black, over the TiO_x rows to highlight the similar periodicity. In both images, the crystal directions correspond to those of the W(100) substrate.

we therefore assign the rows on the TiO_x islands to (1 × 1) rows of TiO_2(110), which have a 6.5 Å periodicity, although we cannot rule out some precursor to these rows. The islands tend to be extended in the direction of these rows. As such, the orientation of the TiO_2(110) islands during the initial growth stages appears to be dictated by the orientation of the W(100)-O(2 × 1) domains.

Figure 4 shows large-area STM images taken from a ~2.6 MLE ultrathin TiO_2(110) film. As can be seen, rather than growing as a continuous film, discrete TiO_2 islands form with heights of ~10–15 Å. The image in Figure 4b resolves the (1 × 1) rows of TiO_2(110), and consistent with the LEED data, the TiO_2 rows are aligned in the orthogonal directions of W[001] or W[010]. The rotational domains are up to 250 Å in length, and usually each island is composed of only one rotational domain.

The TiO_2(110) domains are considerably larger than the W(100)-O(2 × 1) domains; this implies that while the orientation of the TiO_2(110) domains is initially dependent on the orientation of the W(100)-O(2 × 1) substrate, further growth of the TiO_2(110) is determined by the orientation of the TiO_2(110) islands already nucleated.

An expanded view of island α is shown in Figure 4c and comprises two rotational domains of TiO_2(110). This is likely to have arisen from coalescence of a number of originally separate islands. Island β contains only one rotational domain and is elongated along the TiO_2 row direction, i.e., the TiO_2[001] direction, as expected from the Wulff construction.[27] On the other hand, island α deviates greatly from the Wulff shape for a single rutile crystal, having an approximately square shape.

dx.doi.org/10.1021/jp409948u | J. Phys. Chem. C XXXX, XXX, XXX–XXX

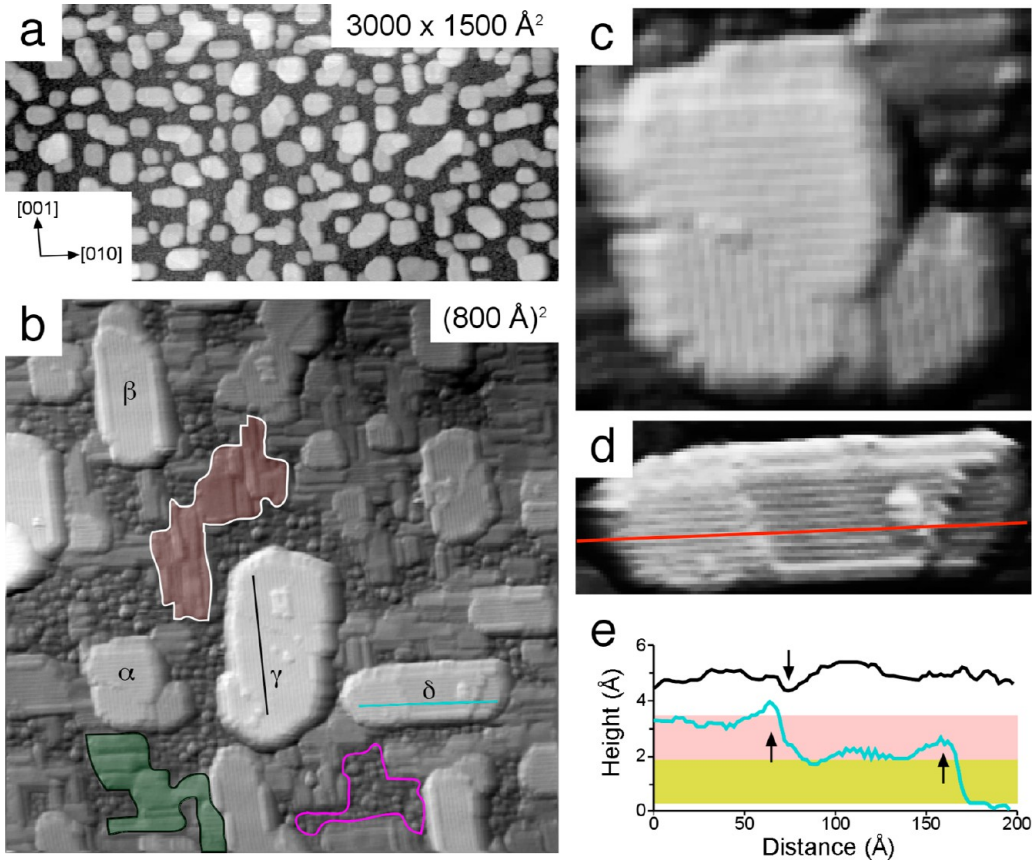

Figure 4. STM images of a ~2.6 MLE TiO_2(110) film on W(100)-O(2 × 1). (a) 3000 × 1500 Å^2 image taken at 1.2 V and 0.1 nA. (b) (800 Å)^2 image taken at 1.5 V and 0.1 nA. A shadow has been applied to the image using Image SXM to enhance the clarity of the atomic-scale row structure. Four large rutile TiO_2(110) islands are labeled *α*, *β*, *γ*, and *δ*. A cluster of smaller rutile TiO_2(110) rods aligned to [010] is enclosed by a black line and shaded green. A similar cluster of rutile rods aligned to [001] is enclosed by a white line and shaded red. An area assigned to the W(100)-O(2 × 1) substrate is outlined in pink. A black line is drawn over island *γ* and a light-blue line is drawn over island *δ*. These lines indicate the positions of the line profiles shown in (e). (c) Magnified view of island *α*, highlighting the rotational domains present. (d) Magnified view of island *δ*, containing a red guideline that runs along a Ti_{5c} row from each of the three terraces. The guideline shows that the rows are in-phase across the step edges. The azimuths shown in (a) apply to all images and correspond to the directions of the W(100) substrate. (e) Line profiles over the positions indicated in (b) but taken from the original unfiltered image. The regions shaded yellow and pink indicate heights of 1.6 Å. Arrows indicate the trench in the line profile of island *γ* and the step edges in island *δ*.

There is also evidence that islands coalesce even when a TiO_2(110) island is composed of just one rotational domain. The black and light-blue line profiles shown in Figure 4e are taken from islands *γ* and *δ*, respectively, as indicated in Figure 4b. The terraces on either side of the apparent step in island *γ* have essentially the same height, and the apparent step is in fact a trench (indicated with an arrow in the line profile). This trench probably arises from a twin boundary introduced when two initially separate islands coalesced during their growth.

As for the line profile from island *δ*, this shows two steps (indicated with arrows in the figure), both of which have heights of about ~1.6 Å. This is significantly lower than the ~3.25 Å step height of a perfect bulk-truncated surface. A step height of ~1.6 Å can be obtained by considering a TiO_2(110) island originating from different W(100)-O(2 × 1) terraces as shown in Figure 5. Such an island could have a range of step heights that take into account the W(100)-O(2 × 1) step of 1.58 Å.[28] Two of these heights are very close to the ~1.6 Å measured: (i) a step edge that directly reflects the substrate step height (1.58 Å) and (ii) a step edge that is equivalent to one step of W(100)-O(2 × 1) subtracted from one step of TiO_2(110), giving a step height of 1.67 Å.

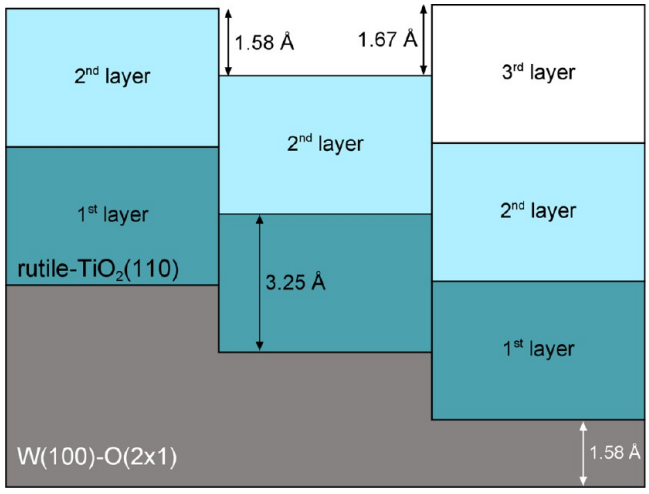

Figure 5. Schematic model showing two of the steps closest to 1.6 Å in height that can arise on the TiO_2(110) island by stacking TiO_2(110) units onto a W(100)-O(2 × 1) substrate. Units of TiO_2(110) are 3.25 Å in height, and steps on the W(100)-O(2 × 1) substrate are 1.58 Å high.

dx.doi.org/10.1021/jp409948u | J. Phys. Chem. C XXXX, XXX, XXX−XXX

The height of these steps are about half that of a normal $TiO_2(110)$ step, which is also characteristic of step edges in the presence of crystallographic shear planes (CSPs). Such CSPs have been observed previously on both native rutile $TiO_2(110)$ surfaces[29−31] and a rutile $TiO_2(110)$ film grown on Ni(110).[15] Normally, CSP formation is caused by reduction of the crystal. As the concentration of oxygen vacancies increases, they order into specific planes that result in the crystal collapsing by slipping half a unit cell along the CS plane. Both step edges on island δ run in the ⟨111⟩ directions, and CSP intersections with (110) have been found along these ⟨111⟩ directions.[15,29−31] A final requirement for assignment of these steps to CSP intersections lies in the alignment of Ti_{5c} rows across the steps: while the Ti_{5c} rows should be *out*-of-phase across normal $TiO_2(110)$ steps, these rows should be *in*-phase across CSP steps. Figure 4d shows an expanded view of island δ. The guideline shows that the Ti_{5c} rows remain in-phase across both step edges. We therefore conclude that both step edges on this island result from the formation of CSPs.

When the density of CSPs is high, arrays of CSP steps form at the surface leading to an "up−down" or "staircase" arrangement.[15,29] The CSPs here are far less dense: only islands β and δ contain them, and even then island β contains only one and island δ two. As such, we propose that rather than being formed by reduction of the crystal, the CSPs here arise as a way of incorporating the ∼1.6 Å steps introduced by the W(100)-O(2 × 1) substrate.

Between these relatively large, well-defined islands are smaller rods that tend to be bunched together. These rods are elongated in the W[001] (red shading/white outline) and W[010] (green shading/black outline) directions. Because some of the flatter rods have rows that are resolved in STM consistent with rutile $TiO_2(110)$ (1 × 1) rows, we assign them as rutile $TiO_2(110)$-(1 × 1) rods. These rods are only about one or two $TiO_2(110)$ layers in height. Some areas, such as that outlined in pink, contain much smaller particles that we assign to the W(100)-O(2 × 1) substrate. We note also that we cannot definitely rule out migration of tungsten-related species into or onto the rods or the larger islands. However, the appearance in STM is consistent with a pure $TiO_2(110)$ termination.

A high-resolution image of the film is shown in Figure 6a alongside a similar image taken from a native $TiO_2(110)$ surface (Figure 6b). The atomic-scale details are indistinguishable. Both images are characterized by bright rows that run along the TiO_2[001] direction with a periodicity of 6.5 Å and are decorated with bright spots that lie between the bright rows. The bright rows are known to correspond to Ti_{5c} rows, and the bright spots are the point defects that may be either O_b-vacs or OH_b.[9,10]

The ultrathin film grown on W(100)-O(2 × 1) has some clear advantages compared to other such films. Our results together with the previous data[19−22] indicate that a single-phase rutile $TiO_2(110)$ film forms on W(100)-O(2 × 1) without any buffer layer. This is in contrast to the TiO_2 films grown on $Ni_{94}Ti_6(110)$, Ni(110), and Ag(100) where multiple TiO_2 phases coexist.[11−14,18] Furthermore, in the case of Ni(110),[14] the rutile islands are thought to grow on top of a lepidocrocite-like TiO_2 wetting layer [first identified on (1 × 2)-Pt(110)],[32,33] and this is also a possibility for Ag(100).[18] It should be noted, however, that coalescence of initially separate islands leads to twin boundaries, including those between orthogonally oriented domains. Such features could affect the overall reactivity of the ultrathin film compared to the native single-crystal surface.

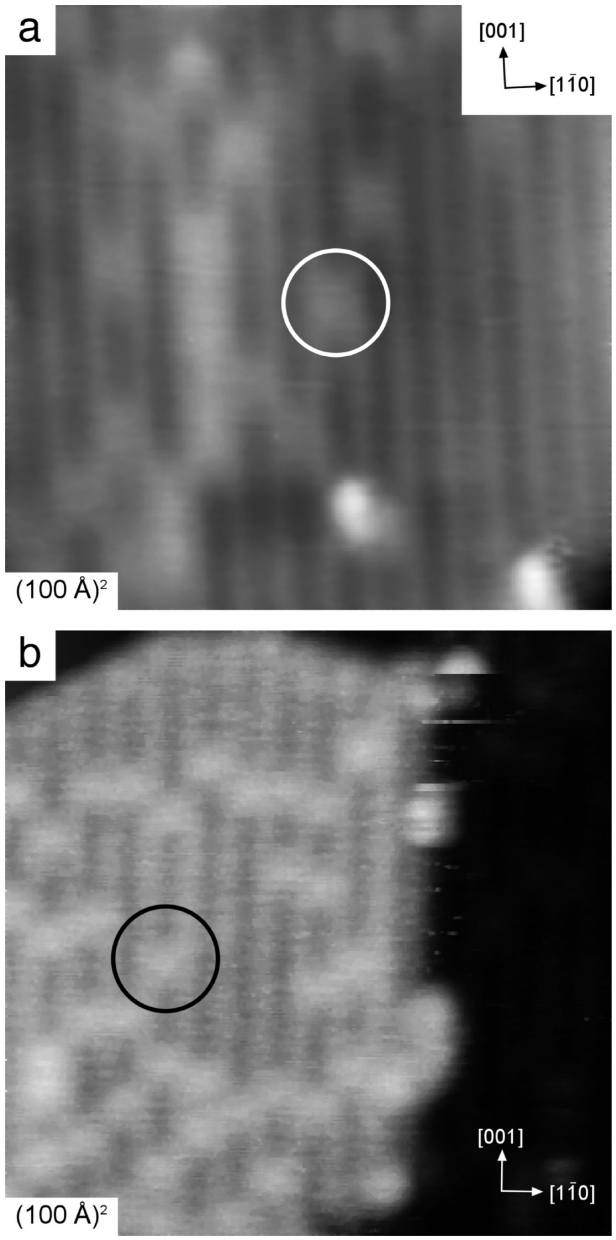

Figure 6. (a) (100 Å)^2 STM image taken at 1.5 V and 0.1 nA from a ∼2.6 MLE $TiO_2(110)$ film on W(100)-O(2 × 1). Atomic-scale bright rows run in the TiO_2[001] direction with a periodicity of ∼6.5 Å. Between these bright rows are a number of bright spots, one of which is marked. The image is consistent with those taken from the native single-crystal $TiO_2(110)$-(1 × 1) surface, an example of which is shown in (b). (b) (100 Å)^2 STM image taken at 1.3 V and 0.1 nA from a native single-crystal $TiO_2(110)$-(1 × 1) surface. Bright rows with a periodicity of 6.5 Å are also observed running in the TiO_2[001] direction between which are a number of bright spots, one of which is marked. In both images, the crystal directions correspond to those of $TiO_2(110)$.

4. CONCLUSIONS

We have grown ultrathin films of rutile $TiO_2(110)$ on a W(100)-O(2 × 1) surface and characterized them with a combination of STM and LEED. The LEED data showed that the rutile $TiO_2(110)$ islands are aligned in both principal

dx.doi.org/10.1021/jp409948u | J. Phys. Chem. C XXXX, XXX, XXX−XXX

directions of the underlying W(100)-O(2 × 1) substrate. STM shows that the (1 × 1) rows of rutile TiO_2(110) are oriented in two orthogonal directions, confirming the observation from LEED. The images also show that rather than forming a continuous film, rutile TiO_2(110) grows as discrete islands. The majority of these islands comprise just one rotational domain of TiO_2(110), although some islands contain both rotational domains due to coalescence of initially separate islands during the growth process. High-resolution STM images show the presence of point defects on the rutile islands that are characteristic of the native rutile TiO_2(110)-(1 × 1) surface.

AUTHOR INFORMATION

Corresponding Author

*London Centre for Nanotechnology, University College London, 17-19 Gordon Street, London WC1H 0AH, U.K. Tel: +44 (0)20 7679 7979. Fax: +44 (0)20 7679 0595. E-mail: g.thornton@ucl.ac.uk.

Notes

The authors declare no competing financial interest.

ACKNOWLEDGMENTS

This work was supported by the EU COST Action CM1104, the European Research Council Advanced Grant ENERGY-SURF (GT), the Royal Society (U.K.), Alexander von Humboldt Stiftung (Germany), and EPSRC (U.K.).

REFERENCES

(1) Franchy, R. Growth of Thin, Crystalline Oxide, Nitride and Oxynitride Films on Metal and Metal Alloy Surfaces. *Surf. Sci. Rep.* **2000**, *38*, 195−294.

(2) Kuhlenbeck, H.; Shaikhutdinov, S.; Freund, H.-J. Well-Ordered Transition Metal Oxide Layers in Model Catalysis − A Series of Case Studies. *Chem. Rev.* **2013**, *113*, 3986−4034.

(3) Grinter, D. C.; Yim, C. M.; Pang, C. L.; Santos, B.; Menteş, T. O.; Locatelli, A.; Thornton, G. Oxidation State Imaging of Ceria Island Growth on Re(0001). *J. Phys. Chem. C* **2013**, *117*, 16509−16514.

(4) Shin, H. J.; Jung, J.; Motobayashi, K.; Yanagisawa, S.; Morikawa, Y.; Kim, Y.; Kawai, M. State-Selective Dissociation of a Single Water Molecule on an Ultrathin MgO Film. *Nat. Mater.* **2010**, *9*, 442−447.

(5) Sterrer, M.; Fischbach, E.; Risse, T.; Freund, H.-J. Geometric Characterization of a Singly Charged Oxygen Vacancy on a Single-Crystalline MgO(001) Film by Electron Paramagnetic Resonance Spectroscopy. *Phys. Rev. Lett.* **2005**, *94*, 186101.

(6) Freund, H.-J.; Pacchioni, G. Oxide Ultra-Thin Films on Metals: New Materials for the Design of Supported Metal Catalysts. *Chem. Soc. Rev.* **2008**, *37*, 2224−2242.

(7) *Metal Oxide Catalysis*; Jackson, S. D., Hargreaves, J. S. J., Eds.; Wiley-VCH: Weinheim, Germnay, 2008.

(8) Diebold, U. The Surface Science of Titanium Dioxide. *Surf. Sci. Rep.* **2003**, *48*, 53−229.

(9) Pang, C. L.; Lindsay, R.; Thornton, G. Structure of Clean and Adsorbate-Covered Single-Crystal Rutile TiO_2 Surfaces. *Chem. Rev.* **2013**, *113*, 3887−3948.

(10) Henderson, M. A.; Lyubinetsky, I. Molecular-Level Insights into Photocatalysis from Scanning Probe Microscopy Studies on TiO_2(110). *Chem. Rev.* **2013**, *113*, 4428−4455.

(11) Atrei, A.; Bardi, U.; Rovida, G. Structure and Composition of the Titanium Oxide Layers Formed by Low-Pressure Oxidation of the $Ni_{94}Ti_6$(110) surface. *Surf. Sci.* **1997**, *391*, 216−225.

(12) Ashworth, T. V.; Thornton, G. Thin Film TiO_2 on Nickel(110): An STM study. *Thin Solid Films* **2001**, *400*, 43−45.

(13) Ashworth, T. V.; Muryn, C. A.; Thornton, G. Nanodots and Other Low-Dimensional Structures of Titanium Oxides. *Nanotechnology* **2005**, *16*, 3041−3044.

(14) Papageorgiou, A. C.; Cabailh, G.; Chen, Q.; Resta, A.; Lundgren, E.; Andersen, J. N.; Thornton, G. Growth and Reactivity of Titanium Oxide Ultrathin Films on Ni(110). *J. Phys. Chem. C* **2007**, *111*, 7704−7710.

(15) Papageorgiou, A. C.; Pang, C. L.; Chen, Q.; Thornton, G. Low-Dimensional, Reduced Phases of Ultrathin TiO_2. *ACS Nano* **2007**, *1*, 409−414.

(16) Guo, Q.; Oh, W. S.; Goodman, D. W. Titanium Oxide Films Grown on Mo(110). *Surf. Sci.* **1999**, *437*, 49−60.

(17) Lai, X.; Guo, Q.; Min, B. K.; Goodman, D. W. Synthesis and Characterization of Titania Films on Mo(110). *Surf. Sci.* **2001**, *487*, 1−8.

(18) Atrei, A.; Cortigiani, B.; Ferrari, A. M. Epitaxial Growth of TiO_2 Films with the Rutile (110) Structure on Ag(100). *J. Phys.: Condens. Matter* **2012**, *24*, 445005.

(19) McCavish, N. D.; Bennett, R. A. Ultra-Thin Film Growth of Titanium Dioxide on W(1 0 0). *Surf. Sci.* **2003**, *546*, 47−56.

(20) Bennett, R. A.; McCavish, N. D. Non-Stoichiometric Oxide Surfaces and Ultra-Thin Films: Characterisation of TiO_2. *Top. Catal.* **2005**, *36*, 11−19.

(21) Bennett, R. A.; Mulley, J. S.; Newton, M. A.; Surman, M. Spectroscopy of Ultrathin Epitaxial Rutile TiO_2(110) Films Grown on W(100). *J. Chem. Phys.* **2007**, *127*, 084707.

(22) Matharu, J.; Cabailh, G.; Thornton, G. Synthesis of TiO_2(110) Ultra-Thin Films on W(100) and their Reactions with H_2O. *Surf. Sci.* **2013**, *616*, 198−205.

(23) Chang, G. S.; Kurmaev, E. Z.; Boukhvalov, D. W.; Finkelstein, L. D.; Kim, D. H.; Noh, T.-W.; Moewes, A.; Callcott, T. A. Clustering of Impurity Atoms in Co-Doped Anatase TiO_2 Thin Films Probed With Soft X-Ray Fluorescence. *J. Phys.: Condens. Matter* **2006**, *18*, 4243−4251.

(24) Bauer, E.; Poppa, H.; Viswanath, Y. Adsorption of Oxygen on W(100): Adsorption Kinetics and Structure. *Surf. Sci.* **1976**, *58*, 517−549.

(25) Meyer, J. A.; Kuk, Y.; Estrup, P. J.; Silverman, P. J. Atomic structure of the high-temperature O/W(001)-(2 × 1) surface. *Phys. Rev. B: Condens. Matter Mater. Phys.* **1991**, *44*, 9104−9107.

(26) Yamazaki, H.; Kamisawa, T.; Kokubun, T.; Haga, T.; Kamimizu, S.; Sakamoto, K. Structure Analysis of Oxygen-Adsorbed Tungsten (001) Surface. *Surf. Sci.* **2001**, *477*, 174−178.

(27) Ramamoorthy, M.; Vanderbilt, D.; King-Smith, R. D. First-Principles Calculations of the Energetics of Stoichiometric TiO_2 Surfaces. *Phys. Rev. B: Condens. Matter Mater. Phys.* **1994**, *49*, 16721−16727.

(28) Murphy, S.; Manai, G.; Shvets, I. V. Oxygen-Induced $p(3 \times 1)$ Reconstruction of the W(100) Surface. *Surf. Sci.* **2005**, *579*, 65−72.

(29) Bennett, R. A.; Poulston, S.; Stone, P.; Bowker, M. STM and LEED Observations of the Surface Structure of TiO_2(110) following Crystallographic Shear Plane Formation. *Phys. Rev. B: Condens. Matter Mater. Phys.* **1999**, *59*, 10341−10346.

(30) Bennett, R. A. The Re-Oxidation of the Substoichiometric TiO_2(110) Surface in the Presence of Crystallographic Shear Planes. *PhysChemComm* **2000**, *3*, 9−14.

(31) McCarty, K. F.; Bartelt, N. C. The 1 × 1/1 × 2 Phase Transition of the TiO_2(110) surface—Variation of Transition Temperature with Crystal Composition. *Surf. Sci.* **2003**, *527*, L203−L212.

(32) Orzali, T.; Casarin, M.; Granozzi, G.; Sambi, M.; Vittadini, A. Bottom-Up Assembly of Single-Domain Titania Nanosheets on (1 × 2)-Pt(110). *Phys. Rev. Lett.* **2006**, *97*, 156101.

(33) Agnoli, S.; Orzali, T.; Sambi, M.; Vittadini, A.; Casarin, M.; Granozzi, G. Ultrathin TiO_2 Films on (1 × 2)-Pt(110): A LEED, Photoemission, STM, and Theoretical Investigation. *J. Phys. Chem. C* **2008**, *112*, 20038−20049.